PERGAMON

Computers and Structures 78 (2000) 185–190

Computers & Structures

www.elsevier.com/locate/compstruc

Buckling of stretched strips

N. Friedl [a,*], F.G. Rammerstorfer [a], F.D. Fischer [b]

[a] *Institute of Lightweight Structures and Aerospace Engineering, Vienna University of Technology, Gusshausstr. 27029/E317, A-1040 Vienna, Austria*

[b] *Institute of Mechanics, University for Mining and Metallurgy, Leoben, Austria*

Received 30 October 1998; accepted 20 October 1999

Abstract

Flat plates subjected to tensile loads may buckle locally in the presence of geometric discontinuities such as cracks, holes or varying dimensions [Shaw D, Huang YH. Buckling behavior of a central cracked thin plate under tension. Engng Fract Mech 1990;35(6):1019–27; Gilabert A, et al. Buckling instability and pattern around holes or cracks in thin plates under tensile load. Eur J Mech A Solids 1992;11(1):65–89; Shimizu S, Yoshida S. Buckling of plates with a hole under tension. Thin-Walled Struct 1991;12:35–49; Tomita Y, Shindo A. Onset and growth of wrinkels in thin square plates subjected to diagonal tension. Int J Mech Sci 1988;30(12):921–31]. However, it appears to be surprising that even in the absence of any geometric discontinuity, buckling due to global tension occurs as a result of special boundary conditions. This effect can be observed during the stretching of thin strips, where high wave number buckling modes can affect large areas. In order to study this phenomenon and to find explanations, computational and analytical investigations were performed. A novel diagram for buckling coefficients is presented, enabling the determination of critical longitudinal stresses.

Keywords: Plate buckling; Buckling coefficients; Stability; Wrinkling

1. Introduction

The literature dealing with buckling under global tension concentrates on the influence of cracks [1,2] and holes [2,3]. In these cases, compressive stresses appear near the defect, because of a local disturbance of the stress field. In the case of cracks, local buckling can increase the speed of crack propagation.

In Ref. [4], a thin square plate subjected to diagonal tension is investigated. The loads are applied at two opposite corners, leading to an inhomogenous stress field and plate buckling perpendicular to the loading direction.

However, also in the absence of geometric discontinuities, buckling due to global tension can occur. In this case, special boundary conditions, constraining the lateral contraction due to the Poisson's effect, lead to lateral compressive stresses at some distance from the boundary. In thin plates, this effect can cause wrinkling. This issue is important during the production of thin metal or plastic sheets. High wave number buckling modes might cause permanent deformations in the plate, reducing the quality of the product.

The aim of this paper is to explain the phenomenon of compressive stresses. Furthermore, analytical estimates and results of numerical analyses are given and the influence of the ratio of plate length to width is discussed.

Critical buckling stresses for plate buckling under global compression or shear can easily be calculated with the help of buckling coefficients taken from diagrams. In the case of global tension, a similar procedure is possible and a novel diagram for buckling coefficients is presented.

* Corresponding author.

0045-7949/00/$ - see front matter
PII: S0045-7949(00)00072-9

2. Mechanical explanation of the phenomenon

The occurrence of compressive lateral stresses in a flat plate under longitudinal tension will be explained for a long plate with the ratio $L/B \geqslant 5.0$ (Fig. 1).

2.1. Long plate under tension

The short edges are clamped, preventing the lateral displacement due to the Poisson's effect (Fig. 1). The two long edges are completely free. The stress field (plane stress) shows two symmetries, thus only one quarter of the plate will be considered in this section (upper left quarter in Fig. 1). It is important to mention that shear stresses vanish along the symmetry lines. In order to find a simple explanation for the compressive stresses, it is useful to split the loading of the linear-elastic problem into two parts. The final result can be found by superposition.

2.1.1. Load case 1: uniaxial tension

In the first step, we apply global tension but allow lateral displacements along the short edges. This will cause an uniform uniaxial stress state. The lateral contraction (in y-direction) is

$$v(y) = -\frac{\sigma_{xx} \nu y}{E} \tag{1}$$

with v as the lateral displacement, σ_{xx}, global tensile stress, ν, Poisson's ratio, y, coordinate in lateral direction, and E, Young's modulus.

The extreme value of the lateral displacement can be found at the free edge ($y = B/2$):

$$v_{\max} = -\frac{\sigma_{xx} \nu B}{2E}. \tag{2}$$

2.1.2. Load case 2: effect of clamped edge

In the second load case, the lateral displacement calculated for the uniaxial case is applied to the "clamped" edge ($x \equiv 0$) with reversed sign. As already mentioned, the superposition of both stress fields will give the solution to the total problem. This solution is

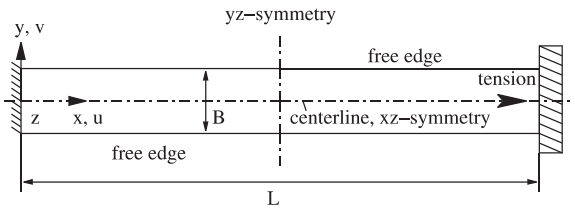

Fig. 1. Long plate.

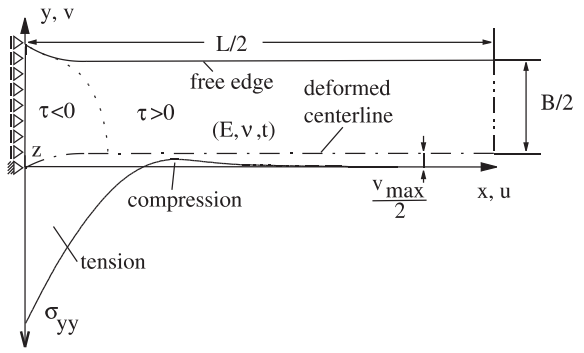

Fig. 2. Quarter of plate.

characterized by a homogenous global component and a local disturbance, which causes the compressive lateral stresses and decays in the longitudinal (x) direction. Hence, long plates fulfill the symmetry condition at the yz-plane automatically (right vertical line in Fig. 2).

In order to find the stresses for load case 2, it is helpful to temporarily consider the centerline ($y \equiv 0$) to be a free boundary. The lateral displacement is applied at the left edge (Fig. 2, $x \equiv 0$). The deformed shape is shown in Fig. 2. The deformed centerline (dash-dotted in Fig. 2) shows zero lateral displacement at the clamped edge ($x \equiv 0$) and a constant value of $v_{\max}/2$ at a sufficient distance from the origin. Since the quarter of the plate is held only on the left side and all other edges are free or temporarily cut free, respectively, the situation can be compared to a cantilever plate.

Now, we can apply the necessary lateral load (lateral stress σ_{yy}) along the lower edge, which moves the deformed centerline back to the x-axis. This stress distribution $\sigma_{yy}(x)$ is shown in a qualitative manner in Fig. 2. Near the clamped edge high lateral stresses are needed to cause local shear deformation in the plate. These lateral tensile stresses also cause bending moments about the z-axis. This would lead to a negative deflection of the cantilever plate, which must be prevented by compressive stresses. The compressive stresses must decay asymptotically in longitudinal direction (Fig. 2).

Although the compressive stresses typically are very small compared to the longitudinal or the lateral tensile stresses, they are responsible for the occurrence of buckling in special configurations. For long plates with a Poisson's ratio of $\nu = 0.3$, finite element studies have shown that the lateral compressive stress is about 0.55% of the global tension. Fig. 3 shows the isolines for the lateral stress component σ_{yy} near the end of a plate with a L/B ratio of 7. The areas with tension and compression, respectively, are divided by the line $\sigma_{yy} = 0.0$. Since the interesting values differ in more than one magnitude, a special scaling is used for the tensile and compressive stresses. In the compression region, the difference between two neighboring lines is approximately fifty times

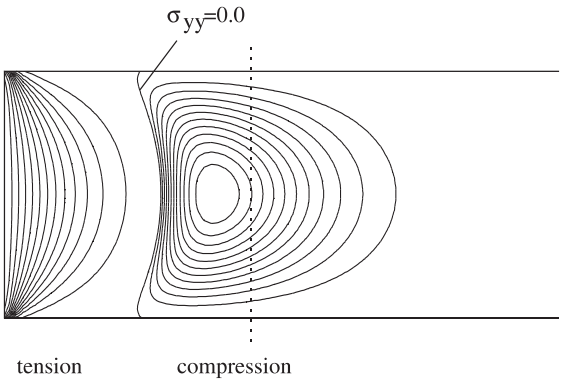

Fig. 3. Isolines of lateral stresses σ_{yy}, $L/B = 7$.

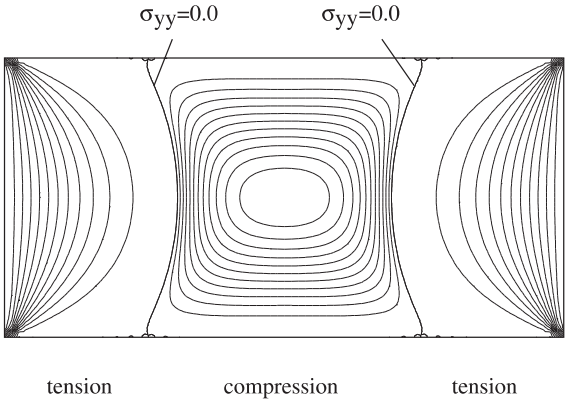

Fig. 5. Isolines of lateral stresses σ_{yy}, $L/B = 2$.

smaller than in the tension region. Absolute values are not important at this point.

Using the cantilever plate model once more, shear is caused by the lateral loading (lateral stresses σ_{yy}). Fig. 4 shows isolines of the shear stresses. Again special scaling is used. The difference between two neighboring lines to the right of point A is approximately 10 times smaller than to the left of A.

Lines with zero shear (symmetry lines) cut the whole plate into four quarters. One edge of each quarter is part of the centerline. Since σ_{yy} changes the sign along the centerline, the shear stresses change their sign in each quarter once again. The isolines of zero shear within the quarter start in point A of Fig. 4 and continue in arcs to the upper and lower free edges (see also Fig. 2, dotted line). The local shear stress maximum and minimum, marked by + and −, occur at the position of the sign reversal of $\sigma_{yy}(x)$ (see Fig. 3, $\sigma_{yy}(x) = 0.0$).

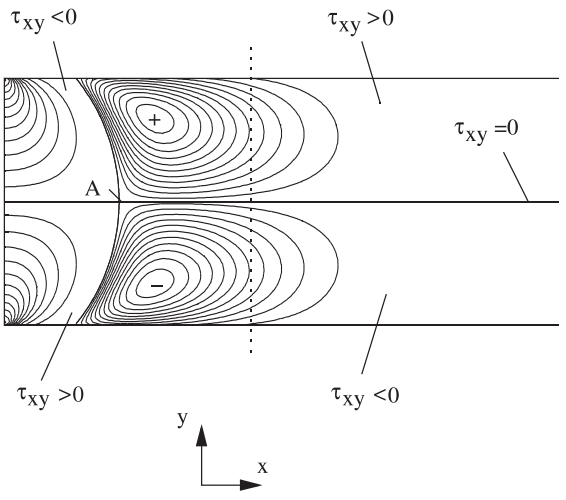

Fig. 4. Isolines of shear stresses τ_{xy}, $L/B = 7$.

2.2. Short plate under tension

In contrast to long plates, for short plates the *yz*-symmetry condition has a great influence on the stress field. If we consider the case, where the *yz*-symmetry lies near the maximum compressive stress of the long plate (vertical dotted line in Figs. 3 and 4), then the shear must vanish at this new symmetry plane. Regarding the upper half of the plate in Fig. 4, the area around the dotted line is dominated by positive shear stresses. Applying the *yz*-symmetry condition at this location is equal to superposing negative shear loading to the solution of the long plate. This negative shear causes additional compressive stresses in the lateral direction. In the lower half, the same mechanism takes place with opposite sign.

For a ratio $L/B = 1.7$ and $v = 0.3$, the maximum lateral compression shows an extreme value of about 1.16% of the global tension, which is more than twice the value of the long plate. Compressive stresses decrease for smaller L/B ratios and vanish for $L/B \leqslant 1.1$. Fig. 5 shows the isolines for the lateral stress component σ_{yy} for a L/B ratio of 2. In this case, the lateral compression is 0.93% of the global tension. The areas with tension and compression are divided by the lines $\sigma_{yy} = 0.0$. Again different scaling for tension and compression is used (see explanation to Fig. 3).

3. Analytical estimates of buckling modes

Prior to the numerical buckling analyses, analytical estimates were performed. However, for the extremely complex stress field no analytical solution for the buckling problem could be found. Hence, in order to

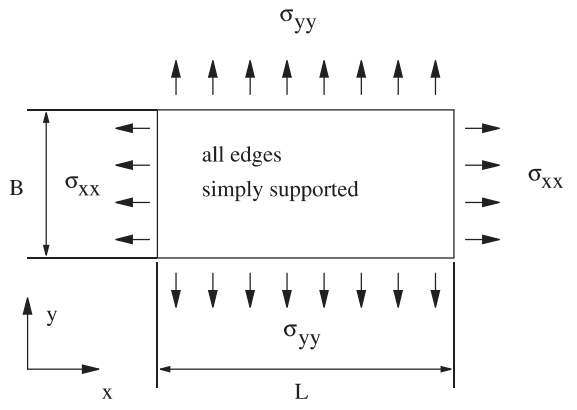

Fig. 6. Simply supported plate.

investigate different effects, it appears to be useful to study the analytical results for a simply supported plate buckling under uniform membrane loads in combined longitudinal and lateral directions (Fig. 6).

For buckling as a result of the Poisson effect, global tension and lateral compression resemble proportional loading. Assuming the same for the analytical model gives:

$$\frac{\sigma_{yy}}{\sigma_{xx}} = C \leqslant 0.0. \tag{3}$$

Then a critical longitudinal stress as a function of the geometry (ratio L/B) and the proportionality factor C can be found:

$$\sigma^*_{xx} = -\frac{\pi^2 E t^2}{12(1-\nu^2)}\left[\frac{\left(\frac{n}{L}\right)^4 + 2\left(\frac{m}{B}\right)^2\left(\frac{n}{L}\right)^2 + \left(\frac{m}{B}\right)^4}{C\left(\frac{m}{B}\right)^2 + \left(\frac{n}{L}\right)^2}\right] \tag{4}$$

with σ^*_{xx} as the critical tensile stress, t, plate thickness, n, half wave number, x direction, and m, half wave number, y direction.

Eq. (4) gives positive values for σ^*_{xx} (tension) when the denominator becomes negative. Normally, the values for L, B and C are known. For the case of buckling under strong longitudinal tensile loading, the half wave number n in the direction of global tension is usually unity for simply supported plates. With this information, a minimum number of half waves $m_{\min}$ in y direction can be found, which is of interest for the discretization of the finite element model:

$$m_{\min} \geqslant \frac{Bn}{L\sqrt{|C|}}. \tag{5}$$

Furthermore, it is important to mention that, at least from a theoretical point of view, a critical tensile stress for any negative C can be found as long as Eq. (5) is satisfied. The global tension is limited by the yield stress or the tensile strength of the material. Reducing the value of $|C|$, i.e. increasing the longitudinal tension load in comparison to the lateral compression load, leads to higher lateral wave numbers.

Looking at the denominator of Eq. (4), we can find a linear stabilizing effect of the global tension only when the term $(n/L)^2$ becomes very small compared to $|C|(m/B)^2$.

4. Numerical buckling analysis

The numerical investigations were performed with the commercial software ABAQUS version 5.7. The shell element S4R5, with reduced integration and hourglass control, was used. The following two geometries are presented:

A: $L = 400$ mm, $B = 200$ mm, $t = 0.05$ mm (Fig. 7A).

B: $L = 1400$ mm, $B = 200$ mm, $t = 0.05$ mm (Fig. 7B).

The material values are the same in both cases: Young's modulus $E = 70\,000$ MPa, Poisson's ratio $\nu = 0.3$. Linear-elastic material behavior is assumed.

In order to find positive eigenvalues for the buckling prediction, a preload close to the critical buckling load is applied, which is similar to an eigenvalue extraction with a shift factor. A simple classical buckling analysis would result in negative eigenvalues describing global compressive stresses in the plate.

The results of the buckling investigations can be seen in Fig. 7. Only the symmetric modes corresponding to the lowest critical tensile stresses are shown. The lowest critical stresses for the antisymmetric modes are identical with those for the symmetric ones. The values of the critical global tensile stresses are 236 MPa for case A and 761 MPa for case B.

The highest compressive stresses occur at a longitudinal distance from the loaded edges of approximately 85% of the plate width B, which holds for all ratios $L/B \geqslant 1.7$. All buckling modes show their largest displacement in those regions. From the regions of the highest lateral compression, the buckles continue in longitudinal direction towards the regions with lateral tensile stress, where they are stopped due to the stabilizing effects. In the case of long plates (Fig. 7B), the buckles continue towards areas with decreasing compressive stresses. The buckles in the mid regions are not a result of the local compressive stresses (which are zero there). Their deformation is caused by the large amplitudes of the buckles at the two end regions in combination with the global tension. The lateral distribution of the compressive stress is nearly parabolic, with the maximum value in the centerline and zero values at the edges. The amplitudes of the buckles decrease rapidly in lateral direction (Fig. 7A and B).

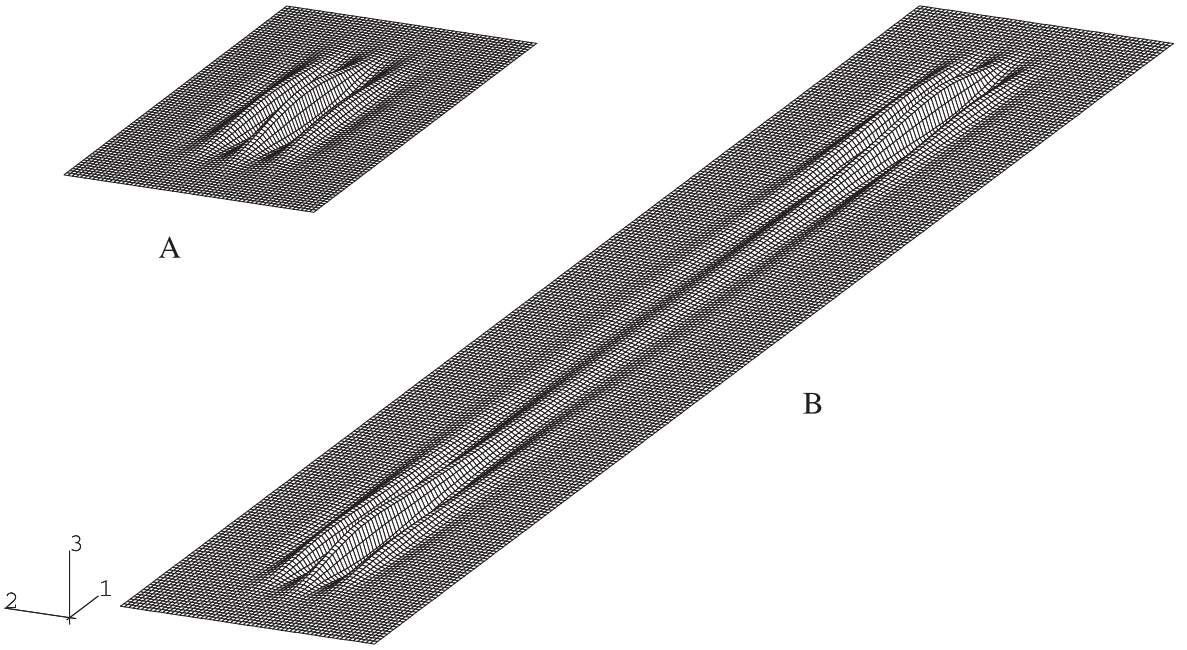

Fig. 7. Buckled plates, A: $L/B = 2$, $\sigma_{11,\mathrm{crit}} = 236$ MPa and B: $L/B = 7$, $\sigma_{11,\mathrm{crit}} = 761$ MPa.

At this point, it is interesting to mention that both plates (Fig. 7A and B) show the same wave number in the lateral direction. Compared to the short plate, the long one has a smaller value of $|C|$ (ratio between maximum lateral compression and global tension). This effect should lead to higher lateral wave numbers. On the other hand, the effective buckling length in longitudinal direction is greater and the stabilizing effect of the boundary is reduced. The combination of both effects seems to cause a constant lateral wave number, independent of the ratio L/B.

5. Simple procedure to determine the critical tensile stresses

In the literature, dealing with the stability of plates under compressive or shear loading, buckling coefficients (k_c, see Eq. (6)) of numerous loading and boundary conditions are defined in diagrams as functions of the ratio L/B. In the case of buckling due to constrained edges, a similar formulation can be derived for tensile loading. Fig. 8 shows the numerically calculated diagram of the buckling coefficients for a fixed Poisson's ratio of 0.3. The buckling coefficients are valid for all materials with linear-elastic, isotropic behavior and the same Poisson's ratio. The critical tensile stress can be calculated in a simple and quick way: The buckling coefficient k_c, a function of the ratio L/B, is taken from the diagram in Fig. 8.

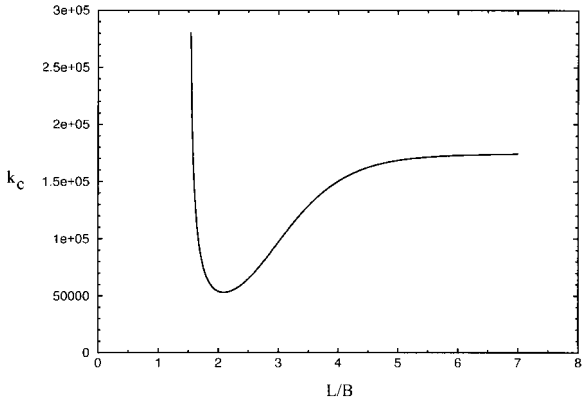

Fig. 8. Critical buckling coefficients.

With the help of Eq. (6), the result is found as

$$\sigma^*_{\mathrm{crit}} = k_c E \left(\frac{t}{B}\right)^2 \tag{6}$$

with σ^*_{crit} as the critical tensile stress, and k_c, buckling coefficient.

The curve of the buckling coefficients (Fig. 8) shows three different significant sections:

(1) $1.5 \leqslant L/B < 2.1$: As already mentioned above, the L/B ratio with the highest lateral compression is approximately 1.7. The minimum buckling factor can be found at $L/B = 2.1$, which means that not only the

magnitude of the compressive stress is important, but also the influence of the boundaries. Moving from the lowest point of the curve ($L/B = 2.1$) to the left, compressive stresses continue to increase (maximum at $L/B = 1.7$), but the effect of the reduction of the buckling length is dominant, and the buckling coefficient increases rapidly. Compressive stresses at the centerline occur for $L/B > 1.1$.

(2) $2.1 \leqslant L/B < 4.5$: Moving from the lowest point ($L/B = 2.1$) to the right, again two opposing effects take place. Both the stabilizing effect of the boundary and the compressive stresses decrease. The compressive stresses dominate the buckling behavior in this area, causing increasing buckling coefficients.

(3) $4.5 \leqslant L/B$: The stabilizing effect of the boundary remains constant, and the compressive stresses in the lateral direction become independent of the plate length L. The influence of the symmetry condition in the yz-plane on the compressive stresses vanishes. The buckling coefficient for $L/B > 7.0$ converges against approximately 175 000.

6. Conclusion

The phenomenon of plate buckling under global tension was discussed for the case in which the instability is a result of the clamped boundary conditions, preventing lateral displacements along the loaded edges. With the means of a simple mechanical model, i.e., a cantilever plate, the origin of the lateral compressive stresses is explained. An analytical investigation of a rectangular plate, simply supported along all four edges, shows the stabilizing effect of the global tension, and minimum half wave numbers in lateral direction can be estimated. Any proportional loading, in which the lateral compression is a constant fraction of the global tension, can theoretically cause buckling. The limits are defined by the yield stress or the tensile strength of the material. Numerically calculated buckling modes for two different L/B ratios are presented. A novel diagram with critical buckling coefficients as a function of the ratio L/B is introduced, allowing the calculation of critical tensile stresses in the same practical way, as used for conventional plate buckling problems.

References

[1] Shaw D, Huang YH. Buckling behavior of a central cracked thin plate under tension. Engng Fract Mech 1990;35(6):1019–27.

[2] Gilabert A, Sibillot P, Sornette D, Vanneste C, Maugis D, Muttin F. Buckling instability and pattern around holes or cracks in thin plates under tensile load. Eur J Mech A Solids 1992;11(1):65–89.

[3] Shimizu S, Yoshida S. Buckling of plates with a hole under tension. Thin-Walled Struct 1991;12:35–49.

[4] Tomita Y, Shindo A. Onset and growth of wrinkels in thin square plates subjected to diagonal tension. Int J Mech Sci 1988;30(12):921–31.